

Multi-ion oscillitons - origin of magnetospheric EMIC waves and further implications

Konrad Sauer¹ and Eduard Dubinin²

¹Retired from MPI for Solar System Research

²Max-Planck-Institute for Solar System Research

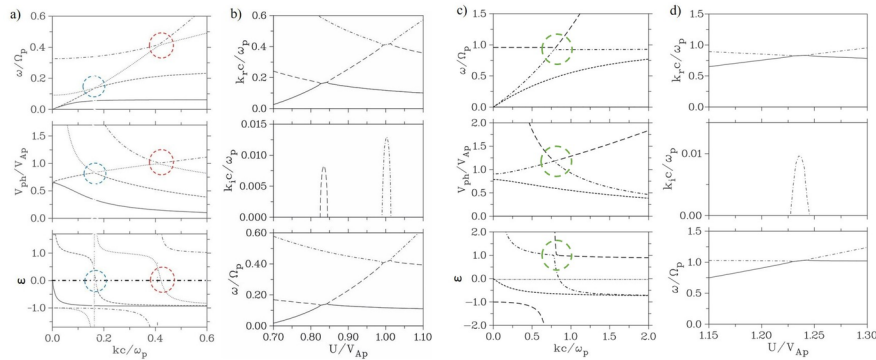
November 26, 2022

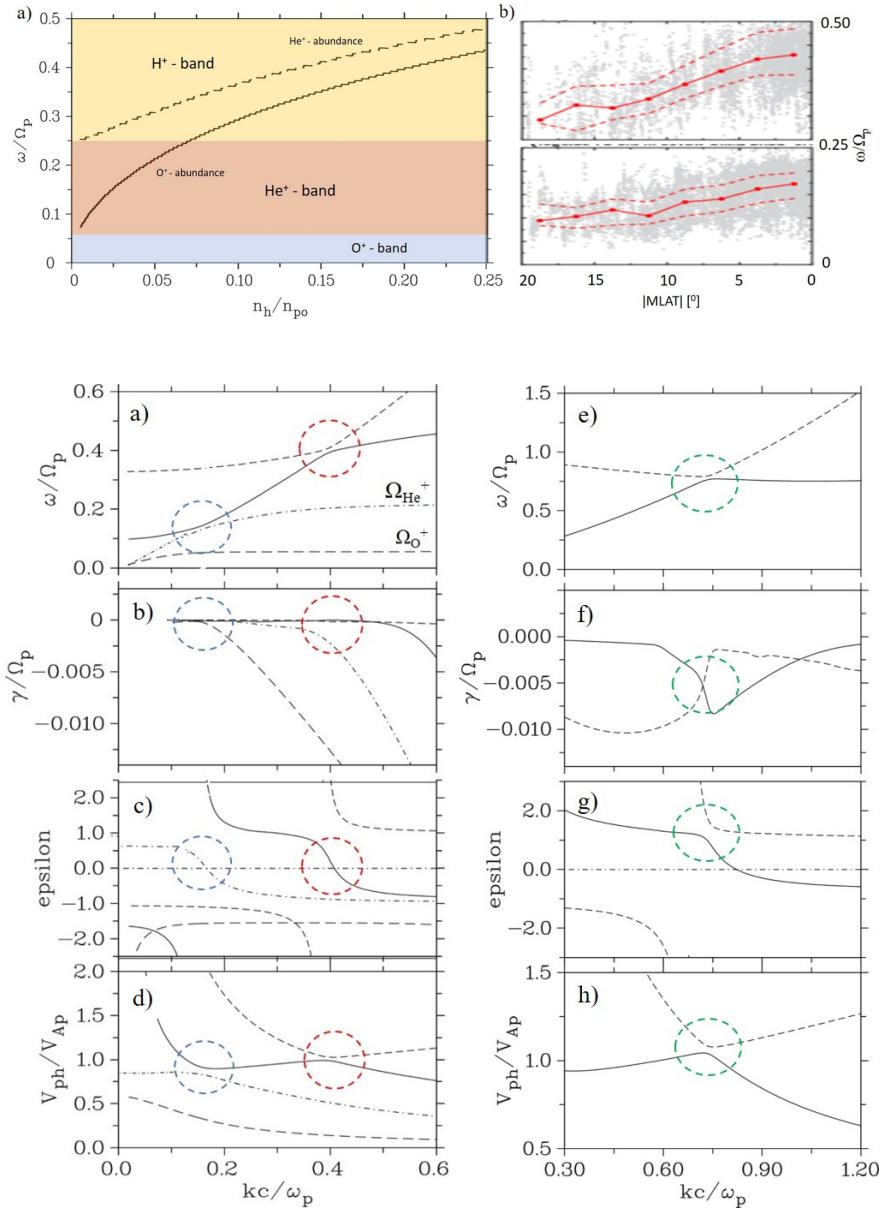
Abstract

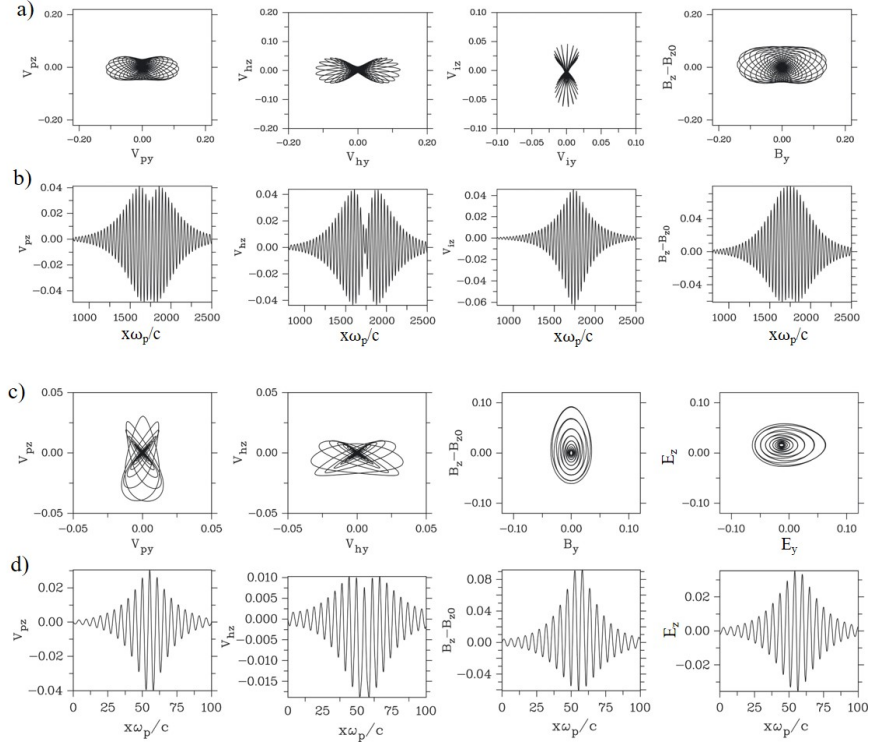
The recent spacecraft observations by MMS and Van Allen Probes associated with electromagnetic ion cyclotron waves (EMIC) in the Earth magnetosphere emphasize the important role of multi-ion plasma composition for generation and characteristics of these emissions. We show that the main properties of EMIC waves can be explained with the concept of ‘multi-ion oscillitons’ (Sauer et al., 2001). In a plasma with two types of ions of different masses (e.g. protons and oxygen ions), oscillitons arise from the exchange of momentum and energy between the two ion components, with the electromagnetic field acting as a mediator. At frequencies near cross-over frequencies of different wave modes in the multi-ion plasma the nonlinear resonance which strongly amplifies the seed unstable mode can be excited. A small phase difference in oscillations of different ion species leads to a nonlinear wave beating and generation of wave packets. The ‘resonance’ frequency is characterized by a local maximum of the phase velocity and the coincidence of phase and group velocity. The generation of coherent waves by oscillitons is of a general nature and may contribute to understand the manifold of phenomena in other space plasma environments in which the dynamics of minor ion admixtures cannot be neglected, as alpha particles in the solar wind and heavy ions around active comets. The concept of oscillitons also applies to the momentum exchange between different particle groups of the same mass. On this way, whistler oscillitons may arise in two-temperature electron plasmas.

Hosted file

essoar.10511652.1.docx available at <https://authorea.com/users/524162/articles/606270-multi-ion-oscillitons-origin-of-magnetospheric-emic-waves-and-further-implications>







Multi-ion oscillitons – origin of magnetospheric EMIC waves and further implications

Konrad Sauer¹ and Eduard Dubinin²

¹*Retired from* Max-Planck Institute of Solar System Research, Göttingen 37077, Germany

²Max-Planck Institute of Solar System Research, Göttingen 37077, Germany

Abstract. The recent spacecraft observations by MMS and Van Allen Probes associated with electromagnetic ion cyclotron waves (EMIC) in the Earth magnetosphere emphasize the important role of multi-ion plasma composition for generation and characteristics of these emissions. We show that the main properties of EMIC waves can be explained with the concept of ‘multi-ion oscillitons’ (Sauer et al., 2001). In a plasma with two types of ions of different masses (e.g. protons and oxygen ions), oscillitons arise from the exchange of momentum and energy between the two ion components, with the electromagnetic field acting as a mediator. At frequencies near cross-over frequencies of different wave modes in the multi-ion plasma the nonlinear resonance which strongly amplifies the seed unstable mode can be excited. A small phase difference in oscillations of different ion species leads to a nonlinear wave beating and generation of wave packets. The ‘resonance’ frequency is characterized by a local maximum of the phase velocity and the coincidence of phase and group velocity. The generation of coherent waves by oscillitons is of a general nature and may contribute to understand the manifold of phenomena in other space plasma environments in which the dynamics of minor ion admixtures cannot be neglected, as alpha particles in the solar wind and heavy ions around active comets. The concept of oscillitons also applies to the momentum exchange between different particle groups of the same mass. On this way, whistler oscillitons may arise in two-temperature electron plasmas.

1. Introduction

Over the last years significant progress has been made in obtaining high-time and spatial resolution of waves in space plasmas. The interesting class of the observed wave emissions is coherent wave structures in the form of wave packets. Examples are near monochromatic packets of right-hand circularly polarized waves (lion roars) (Zhang et al., 1998, Baumjohann et al., 1999, Dubinin et al., 2007), large amplitude quasi-monochromatic ULF waves in the ion foreshock (Fuselier et al., 1986, Fazakerley et al., 1995), narrow-band chorus emissions (Tsurutani and Smith, 1974, Tsurutani et al. 2020). Often such structures are observed in plasmas which contain different ion populations. It was suggested that these waves might represent a new class of solitary waves containing solitons with an embedded smaller scale oscillating core and therefore were called oscillitons (Sauer et al., 2001, 2002, 2003a,b, 2011, Dubinin 2002, 2003a,b,c, 2004). These nonlinear structures are produced by a nonlinear resonance driven by the momentum exchange between the protons and electrons in whistler modes or between an ion beam and the main plasma or between the different ion pop-

ulations in multi-ion plasmas, or even between two proton populations with different temperatures. In all such cases the momentum exchange is mediated by the Maxwell magnetic stresses. It occurs that phases of wave oscillations of the interplaying particles are slightly different that results in a wave beating and creation of wave packets (Dubinin et al., 2003c). It is interesting to note that the existence of such nonlinear structures can be predicted from a dispersion analysis even without the exact solutions. The favorable conditions are realized when the phase velocity exhibits a maximum (inflection point in $-k$ space). For example, for whistlers in a cold plasma it happens at $\omega_{He}/2$. In multi-ion plasma it happens near cross-over frequencies of different wave modes. The feature of this frequency at which the phase and the group velocities are matched is that the wave packets will be bunched up there. Different types of plasma instabilities driven either by a beam or by a temperature anisotropy can excite a broad range of emissions. The mode at which the nonlinear resonance might be excited is selected from the ensemble of the linearly unstable waves and amplified as the system resonates at this frequency.

Electromagnetic ion cyclotron (EMIC) waves bring us another example of coherent wave structures. The improved technology of recent spacecraft missions associated also with multi-point measurements has achieved a wealth of new data about these waves. The new observations emphasize an important role of multi-ion plasma composition for generation and characteristics of EMIC waves. Multi-ion composition is a common feature for space plasmas. Even a small admixture of a second ion component to a proton-electron plasma can significantly change wave characteristics and plasma flows. The presence of a tenuous He⁺⁺ component in solar wind modifies the dispersion of plasma waves and leads to a change of polarization near the cross-over frequency. Such effects were recently observed by the Solar Orbiter (Khotyaintsev et al., 2021). A change in dispersion may result in appearance of a new class of nonlinear waves in the plasma of protons and α -particles (Dubinin et al., 2003a,b). Left-handed MHD waves arising near the cross-over frequency may also be an important agent in the coronal heating of the solar wind (Li and Habbal, 2001). Inclusion of alpha-particles into a proton-electron plasma can also reduce the growth rate of the proton cyclotron instability and control a dominance of ion cyclotron or mirror waves (Gary et al., 1994). Multi-ion component plasmas are also typical for comets where we observe a rich variety of waves and coherent structures (Tsurutani, 1991). Multi-ion origin of plasma is also manifested near Venus and Mars with extended exospheres, or near moons of Jupiter and Saturn.

In this paper, we show that diverse phenomena of EMIC waves can be explained with the concept of ‘multi-ion oscillitons’. The theoretical background of oscillitons in the frequency range of EMIC waves is formed by the multi-ion Hall-MHD equations which are derived from the multi-fluid equations by replacing the electric field via the assumption of mass-less electrons and by using charge neutrality. In general, a three-ion plasma of protons, single charged helium and oxygen is considered. By solving the dispersion relation of cold ions one gets a first survey about the $-k$ position of the cross-over frequencies together with

the k -variation of the wave polarization as function of the abundance ratios and the wave propagation angle. In the next step, the linear characteristics of stationary waves $k=k(U)$ are determined. They represent a useful pre-information in solving the full nonlinear, stationary Hall-MHD equations to get the spatial profiles of oscillitons. Several examples of the calculated wave packets are given. In addition it is shown that oscillitons also exist in multi-ion plasmas where two heavy-ion populations of the same mass but with different temperatures or streaming velocities are present. This leads to oscilliton frequencies very close to heavy-ion cyclotron frequency, in contrast to the more common case where the cross-over frequency is above the cyclotron frequency of the heavy ion population. We also compare the theoretical results with the properties of observed EMIC events in space. Since EMIC waves are more extensively studied near the Earth we make a comparison with recent observations in the Earth magnetosphere. It concerns the frequency, the wave polarization and possible plasma parameters which can be derived from the theoretical model. The influence of kinetic damping due to finite electron and ion temperatures is discussed, too.

1. Theoretical background of oscillitons

According to the magnetospheric conditions, we consider a space plasma which consisting of electrons and three ion populations, protons single-ionized helium and oxygen, here denoted by the indices p for protons, h for He^+ and i for O^+ , respectively. With the proton density n_{p0} as reference, a standard composition of 10% helium ($n_{h0}/n_{p0}=0.1$) and 5% oxygen ($n_{i0}/n_{p0}=0.05$) is assumed. The starting point are the multi-fluid equations which have been used in earlier papers on non-linear stationary waves [Sauer et al., 2001, 2002, 2003a,b, 2011; Dubinin et al., 2002, 2003a,b,c; McKenzie et al., 2004]. They follow in a straightforward way from the usual multi-ion equations by eliminating the electric field by the following assumptions which are relevant to the low-frequency processes under consideration: i) massless electrons and ii) charge neutrality, i.e. $n_e=n_p+n_h+n_i$. This so-called Hall-MHD model is described e.g. by Huba (2003) in detail and has been applied for many purposes in space physics, as for modelling the solar wind interaction with non-magnetized bodies, e.g. Sauer et al. (1994), Nagy et al. (2004) and Rubin et al. (2014). A summary of these equations can be found in Appendix A.

2.1 Multi-ion dispersion theory

In order to analyse the dispersion characteristics of low-frequency waves in multi-ion plasmas, the linearized version of the Hall-MHD equations are solved for plane waves in the common way. The applied tensor formalism is similar as described before by Sauer and Sydora (2010). After Fourier transform (all variables vary as $\sim \exp(-i(\mathbf{k} \cdot \mathbf{x}))$), the fluid and Maxwell equations are written in tensor form which by means of matrix operations of *Mathematica* [Wolfram, 1988] finally leads to the equation

$$\mathbf{M}(\omega, \mathbf{k}) \cdot \mathbf{E}(\omega, \mathbf{k}) = \mathbf{0} \quad (2.1)$$

where \mathbf{M} is the multi-ion dispersion tensor as a function of ω and \mathbf{k} which con-

tains the undisturbed plasma parameters (density, velocity, temperature, mass, charge) of the ion populations in addition to the propagation angle with respect to the magnetic field which was taken in z-direction. From there, one gets the dispersion relation

$$D = \text{Determinant}[\mathbf{M}] = 0. \quad (2.2)$$

It represents a polynomial (with real coefficients) of n-th order in ω as function of k where n depends upon how many particle populations are taken and whether they are considered as cold or warm or a beam population is present. Further, using the matrix relation (2.1), the polarization of the multi-ion waves can easily be calculated. From the three equations for the electric field components E_x , E_y and E_z the polarization (ϵ) is obtained as the ratio $\epsilon = i E_y / E_z$ by simple algebra. Similar dispersion analysis of cold multi-ion plasmas has been done long before, e.g. by Smith and Brice (1964), Rauch and Roux (1982) and Thompson et al. (1995). Our focus of dispersion analysis is mainly directed on the coupling between different wave modes which occurs if the waves propagate oblique to the magnetic field.

In Figure 1, solutions of the dispersion relation (2.2) are shown for two cases. The three panels of Figure 1a belong to a multi-ion plasma consisting of cold protons, single-ionized helium and oxygen with an abundance ratio (with respect to the proton density) of $N_{\text{He}^+} = 10\%$ and $N_{\text{O}^+} = 5\%$. The propagation angle is $\theta = 15^\circ$. The essential effect of interest is the mode splitting between the two kinds of waves, the originally right-hand polarized R-mode and the originally left-hand polarized L-modes which arise due to the heavy-ion abundance. Whereas at parallel propagation these modes cross each other without any effect, frequency gaps arise at the cross-over points (marked by the red and blue dashed circles) if the waves propagate oblique to the magnetic field. Characteristic frequencies which are related to the heavy-ion abundances and needed for later discussion are the two cut-off frequencies (at $k=0$), approximately given by $\omega_{\text{cut1}} \sim \Omega_p (n_{\text{O}^+} / n_p + m_p / m_{\text{O}^+}) = 0.11$ and $\omega_{\text{cut2}} \sim \Omega_p (n_{\text{He}^+} / n_p + m_p / m_{\text{He}^+}) = 0.35$, and the two cross-over frequencies which are located above their related cut-off frequencies. As a remarkable feature, the phase velocity shown in middle panel a) gets a maximum (minimum) at the mode crossing points. As one could imagine and can clearly be seen in the bottom panel, a change of polarization at the cross-over frequencies takes place. For example, the dotted curve which is R-polarized at small wave numbers k changes to linear polarization at the point of maximum phase velocity (marked by the blue dashed circle) and goes with increasing k over to left-hand polarization. A similar behaviour takes place for larger wave numbers at the second cross-over point (red dashed circle) at $(\omega / \Omega_p \sim 0.4, kc / v_p \sim 0.4)$ which is associated with the He^+ abundance. Observation of EMIC waves with linear polarization is partly explained in literature via mode conversion [Young et al., 1981; Jun et al., 2021] when the propagating waves approaches the cross-over point. We come back to this in the discussion.

The second example of multi-ion dispersion analysis, shown in the three panels

of Figure 1c, concerns a case where mode splitting appears due to the existence of two ion populations of the same mass, but with different temperatures. Here, cold and hot proton populations are considered. As we will discuss later, this situation creates requirements of EMIC wave generation very close to the proton cyclotron frequency, or more general, close to the cyclotron frequency of two-temperature heavy ions under consideration. As in Figure 1a from top to bottom the frequency, the phase velocity and polarization are shown. As seen, the mode splitting effects are similar as for EMIC waves in the proton plasma with heavy-ion abundances. At the cross-over (ω, k) point, marked by the green dashed circle, the phase velocity has a maximum (minimum) and changes the polarization there from right- to left-hand polarization (and vice-a versa) .

2.2 Linear stationary waves

A next step in accordance with the approach to oscillitons in the original paper by Sauer et al. (2001) consists in the proof of linear stationary waves in the gap areas around the cross-over points. For this purpose the frequency in the dispersion relation 2.2 is replaced by $\mathbf{k} \cdot \mathbf{U}$ where \mathbf{U} is the velocity of the moving frame. With $\omega = \mathbf{k} \cdot \mathbf{U}$, equation 2.2 is transformed in a polynomial in k as function of the ‘oscilliton velocity’ U . Solutions of the resulting dispersion relation of stationary waves $D(\mathbf{k} \cdot \mathbf{U}, k)=0$ are shown in Figures 1b and 1d. By comparison with the related plots of Figures 1a and 1b one can clearly see that growing stationary waves with $k_i > 0$ (k_i : imaginary part of k) occur just there, where ‘forbidden’ areas in the (ω, k) space owing to mode splitting arise. According to Figure 1b, due to the presence of two heavy ion populations (helium and oxygen), one gets two ranges of ‘oscilliton’ velocities with the related frequencies and (real) wave numbers. For the selected abundance ratios of 5% O^+ and 10% He^+ and a propagation angle of $\theta = 15^\circ$, the associated ‘oscilliton’ frequencies are $0.2\Omega_p$ and $0.45\Omega_p$, respectively. How these frequencies vary with the propagation angle will subsequently be discussed. Figure 1d belongs to the plasma with both a cold and hot proton population. As an essential signature one has to note that for this kind of plasma a growing stationary wave with a frequency close to the proton cyclotron frequency arises. In plasmas with heavy-ion admixtures, on the other hand, a comparable approaching to this frequency cannot be achieved by reasonable abundance ratios.

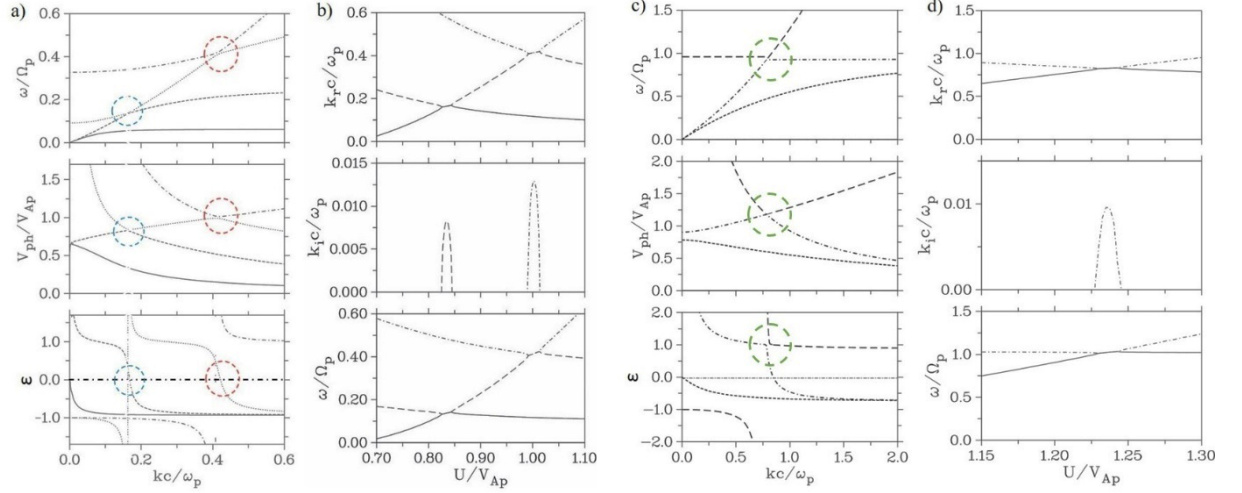


Figure 1. Multi-ion dispersion theory and linear stationary waves, fluid approach. a) The left three panels belong to the cold plasma consisting of electrons, protons, He^+ and O^+ ions. The heavy-ion densities normalized to the proton density are $N_{\text{He}^+}=10\%$ and $N_{\text{O}^+}=5\%$, respectively. The propagation angle is $\theta=15^\circ$. From top to bottom: the (normalized) frequency ω/Ω_p , the (normalized) parallel phase velocity $V_{\text{ph}}/V_{\text{Ap}}$ and the polarization (epsilon) versus the (normalized) wave number kc/ω_p . The dashed blue and red circles mark the cross-over points in the H^+ and He^+ bands, respectively. b) Linear stationary multi-ion waves $k=k(U)$ resulting from the dispersion relation of the propagating waves in a) by the replacement $\omega \rightarrow k \cdot U$ where U is the velocity of the moving frame. From top to bottom: real and imaginary part (spatial growth rate) of the wave number kc/ω_p and the ‘oscilliton frequency’ ω_c/ω_p versus U/V_{Ap} . As seen in the middle panel, growing stationary waves occur at the mode-crossing points. c) The same format as in a) showing the dispersion $\omega(k)$ of a two-temperature plasma of cold and warm protons (relative density $N_{\text{H}^+}=25\%$, $N_{\text{H}^+}=0.25$); $\theta=25^\circ$. The cross-over points are marked by green dashed circles. d) Stationary waves $k=k(u)$ in the two-temperature plasma of Figure 1c. Maximum spatial growth rate (middle panel) appears at the ‘oscilliton frequency’ $\omega_c=k_r \cdot U$ (bottom panel) very close to the proton cyclotron frequency Ω_p .

From the two examples which have been described in Figure 1 it is evident that the analysis of the stationary waves in multi-ion plasmas represents a simple tool in order to get useful predictions for further studies. So, the growth rate of stationary waves can easily be used to determine the associated ‘oscilliton frequency’ in dependence of main parameters, as propagation angle θ , for example, the maximum growth rate is determined versus the abundance ratio (heavy-ion density/proton density) of O^+ and He^+ ions, respectively. From the ‘oscilliton

velocity' U at maximum spatial growth and the associated (real) wave number k_r , one then obtains the 'oscilliton frequency' $\omega = k_r \cdot U$, which according to our general philosophy is almost identical to the corresponding cross-over frequency. Such a dependency is shown in Figure 2 for a fixed propagation angle of $\theta = 15^\circ$, where in the range of small angles ($\theta < 30^\circ$) there are only relatively small shifts in both curves. It is noteworthy that due to He^+ even with moderate admixture ($< 25\%$), the 'oscilliton frequency' remains below $0.5 \Omega_p$. With O^+ , on the other hand, a frequency shift from the He^+ band to the H^+ band can already take place with an addition of less than 10%. As we will discuss, this dependency is directly related to statistical results from satellite measurements., see e.g. Jun et al. (2021).

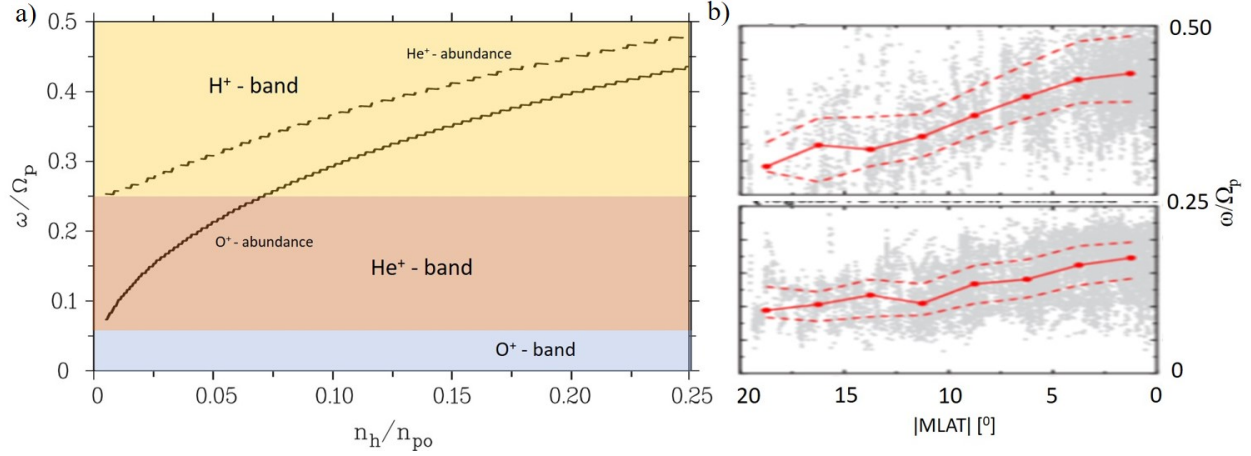


Figure 2. a) ‘Oscilliton frequency’ versus the He^+ (dashed curve) and O^+ abundance ratio (solid curve), respectively, for a fixed propagation angle of $\theta = 15^\circ$. The dependence has been determined from the maximum growth rate of stationary waves $k=k(U)$, whereby only one heavy ion population was considered as an addition to the proton plasma. That means, the index ‘h’ stands for ‘ He^+ ’ and ‘ O^+ ’ separately. b) Statistical Van Allen Probe measurements of the normalized frequency of EMIC waves in the H^+ (upper panel) and He^+ band (lower panel) versus MLAT, adapted from Jun et al. (2019).

2.3 Kinetic dispersion analysis (Vlasov approach)

In order to analyze to what extent the multi-fluid theory results shown in Figures 1a and 1c are influenced by kinetic damping effects, our own code to solve the kinetic dispersion relation was used. This code written on the formalism of Stix (1992) has successfully applied for different purposes. Hereby, the knowledge of the fluid results made it easier to find the corresponding solutions of the Vlasov description. Results for the same parameters as in Figure 1 with respect to the abundance ratios and propagation angles, supplemented by the plasma temperatures of electrons and ions via the related plasma betas β_i ($i = e, \text{H}^+, \text{He}^+, \text{O}^+$) are shown Figure 3. Looking first to the left two panels for the

multi-ion dispersion at presence of protons, helium and oxygen ions, the good agreement between both approaches with respect to the real part of frequency in a), the polarization in c) and the phase velocity in d) is visible. As additional information one gets the kinetic damping in panel b). As a remarkable effect one has to note the onset of significant damping of the left-hand polarized (cyclotron) modes after their crossing of the weakly damped right-hand mode. The right panels e) – h) show the dispersion behavior in the vicinity of the proton cyclotron frequency for the case that the proton plasma consists of a cold ($\beta_c=0.001$) and hot population ($\beta_h=0.02$) whose density is 25% of the cold one. Essential effects are again the pronounced mode splitting between the both modes of different polarization and the associated formation of an inflection point where phase and group velocity coincide.

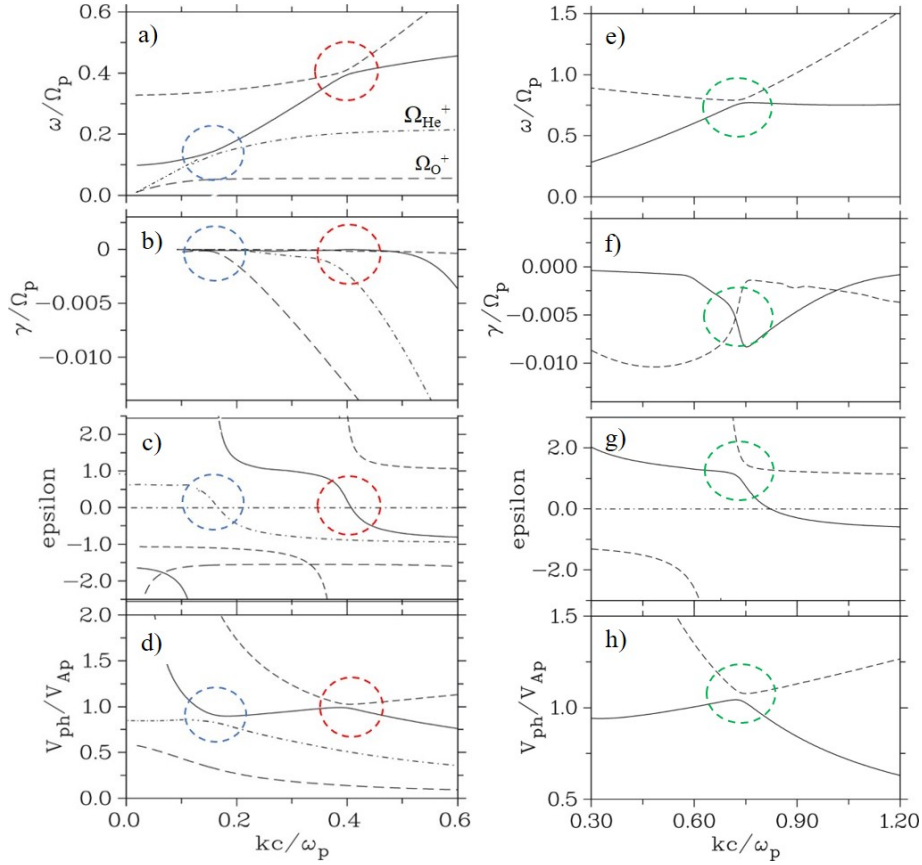


Figure 3. Similar format as in Figure 1, however, instead of fluid theory the Vlasov dispersion relation including kinetic damping by finite electron and ion temperatures has been used. The damping rate γ/Ω_p is added in the second row, panels b) and f). For the multi-ion case (left panels) the temperatures of the ions (H^+ , He^+ and O^+) are given by $\beta_{H^+} = 0.15$ and $\beta_{He^+} = \beta_{O^+} = 0.01$. For the

electrons $n_e=0.2$ was used. The right panels belong to two-temperature plasma of cold ($n_{H^+}=0.001$) and warm protons (relative density $N_{H^+}=25\%$, $n_{H^+}=0.25$); $\theta=25^\circ$.

1. Spatial oscilliton profiles

The final step to oscillitons is the calculation of their spatial profiles by solving the stationary nonlinear fluid equations. The procedure of deriving the governing system of ordinary differential equations is detailed described in earlier papers by Sauer et al. (2001, 2002, 2003a,b, 2011), Dubinin et al. (2002, 2003a,b,c, 2004) and McKenzie et al. (2004) and, therefore, only few explanations are given here. Starting point are the Hall-MHD equations as already explained in section 2.1. In the one-dimensional model the x-direction is determined by the direction of the wave propagation. The y- and z-axes complete the orthogonal system, with the magnetic field lying in the x-z plane and forming the angle θ with the x-axis. The search for stationary waves means switching to the reference system, in which there is no time dependence. That is, $\partial/\partial t$ is replaced by $-U d/dx$, where U stands for the so-called oscilliton velocity. Thus, the complete system of nonlinear equations in x and t is converted into a system of ordinary differential equations. Using in addition the conservation of mass flux and transverse momentum, for a plasma with three ion species (protons, helium and oxygen ions), finally nine equations are required to determine the relevant quantities, i.e. density, velocity of ions and the magnetic field. Essential parameters are the abundance ratios of the heavy ions and the temperatures of electrons and ions, expressed by their plasma betas β_i . They together with the propagation angle θ determine the range of ‘oscilliton velocities’ U in which, according to the linear theory in Section 2.2, spatially increasing solutions with the corresponding spatial growth rates occur. (For the simple case of the cold two-ion plasma, the equations to be solved are given explicitly in Appendix B.)

The following normalizations are used below: The densities relate to the proton density n_{p0} , the velocities are normalized with the proton Alfvén speed V_{Ap} . The magnetic field disturbances refer to the undisturbed magnetic field B_0 and finally the electric fields are normalized with $E_0=V_{Ap} B_0$. As a first example, the spatial profiles are determined for the case that three ion populations take part at the momentum coupling between magnetized ions and the electromagnetic field. As before, a plasma of protons with a proportion of 10% helium (He^+) and 5% oxygen ions (O^+) is assumed. According to the descriptions in the previous sections (Figure 1a, b), such a three-ion plasma has two cross-over frequencies and thus two propagation velocities U at which oscillitons are to be expected. In the context of our fluid model, these are determined by the abundance ratios and the propagation angle. In the following we choose $\theta=15^\circ$ and determine the spatial profiles of the oscilliton in the He^+ band which, according to Figure 1b, exists at $M=U/V_{Ap}=0.83$ with $kc/\omega_e\sim 0.22$ and thus $\omega/\Omega_e=0.18$. The numerical integration of the differential equations describing the spatial oscilliton profiles results in the plots of Figure 4a and 4b. In Figure 4a, the hodograms of the transverse velocities and of the transverse magnetic field are shown, whereby the

index ‘h’ stands for He^+ and ‘i’ for ‘ O^+ ’. The corresponding spatial variation of the z-component of the four quantities is pictured below in Figure 4b. From the hodograms one can see the tendency towards linear polarization and the close correlation between the rotating motion of the ions and the behavior of the magnetic field. Further, it can be seen that there is a 90 degree phase shift between the rotation of O^+ and He^+ .

Of a particular interest is the occurrence of EMIC waves in the immediate vicinity of the cyclotron frequency of an ion species present in the plasma. For example, Teng et al. (2019) describe the generation and characteristics of emission at the proton cyclotron frequency. These particular EMIC events are interpreted as oscillitons which are based on the presence of two populations of the same mass but with different temperatures or drifts. As analyzed in Figures 1c and 1d, mode coupling takes place here between the two components and leads ultimately to the possibility of stationary growing waves. A corresponding example is shown in the panels of Figures 4c and 4d, where the interaction between two proton populations of different temperature generates an oscilliton very close to the proton cyclotron frequency. In the present case it is assumed that the plasma consists of cold protons (index p) with the same admixture of warm protons (index h) with $\beta_h=0.2$. For $\theta=60^\circ$, the oscilliton velocity is $M=0.83$ and with $kc/v_e=1.24$ one gets an ‘oscilliton frequency’ of $\omega/\Omega_p \sim 1$. As can be seen from the first two hodograms in Figure 4c, the two proton groups (‘p’ for the cold population, ‘h’ for the hot one) perform very different gyrating motions, which finally, as a result of the self-consistent interaction, causes the particular polarization of the magnetic field, plotted in the third hodogram. What the different particle gyrations look like in detail depends on the respective parameters of the proton groups. Remarkable is the significant variation of the density of cold ions (not shown here), which reaches almost 10%, which is also similarly reflected in the amplitude variation of the magnetic field. In the fourth panels of Figure 4c the hodogram of the electric field is shown, whereby E_y , E_z are related to B_y , B_z by $E_y=M \cdot (B_z - B_{z0})$ and $E_z=-M \cdot B_y$. In the four panels of Figure 4d, finally, the spatial profiles of the z-component of the proton velocities (V_{pz} and V_{hz}), of the magnetic field ($B_z - B_{z0}$) and of the electric field (E_z) are pictured. As will be shown later, the mutual drift of two particle populations of the same mass and temperature can lead to similar effects.

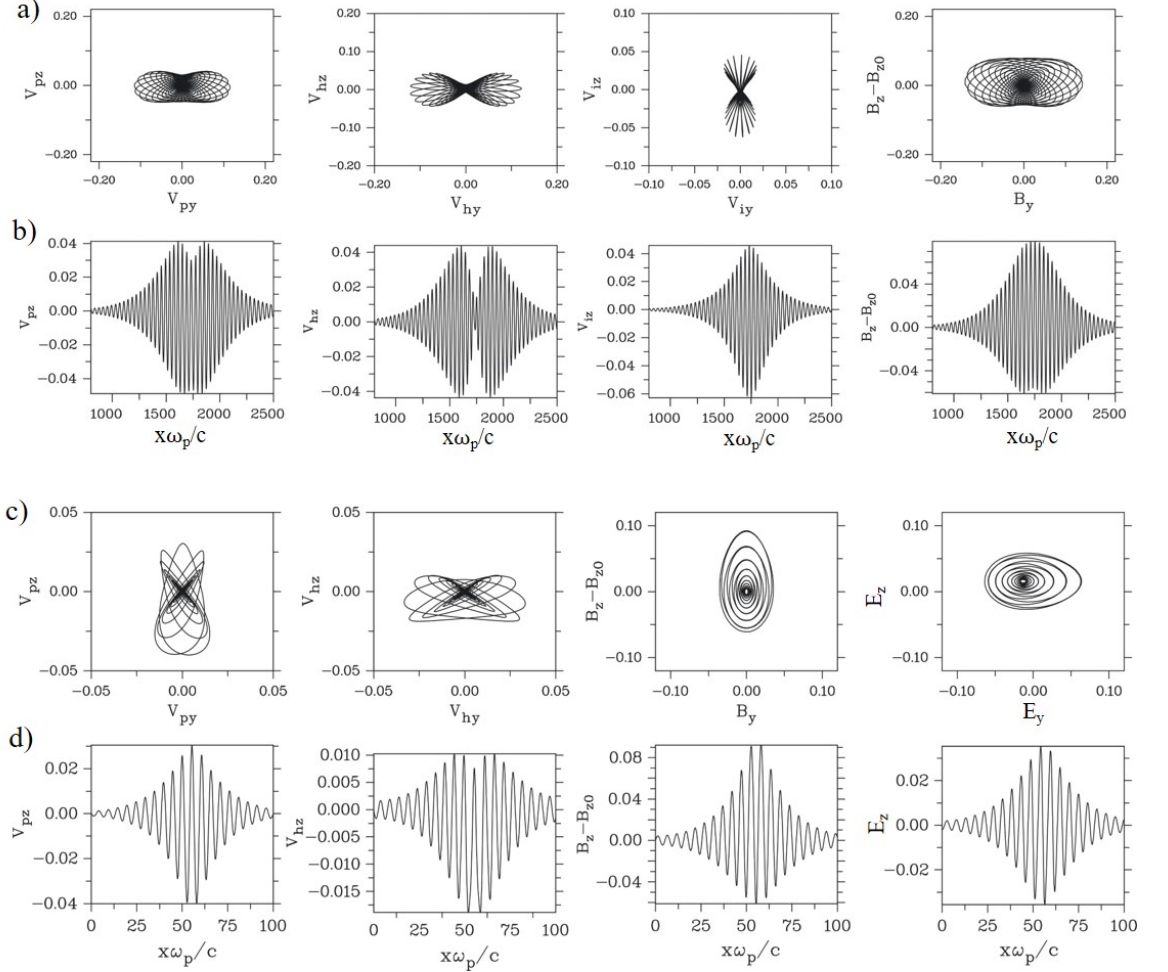


Figure 4. Hodograms and spatial profiles of oscillitons: a), b) Multi-ion plasma consisting of three (cold) ion populations: protons, He^+ -ions (10% of the proton density) and O^+ -ions (5% of the proton density). The oscilliton moves with the velocity $M=0.83$ which corresponds to a frequency of $\omega/\Omega_p=0.18$. The propagation angle is $\theta=15^\circ$. The panels of Figure 4a shows the hodograms of the transverse velocities (indicies: p for protons, h for He^+ ions and i for O^+ ions) and of the transverse magnetic field. The corresponding spatial oscilliton profiles are shown in Figure 4b. The plots in Figure 4c and 4d belong to a two-temperature proton plasma which consists of a cold (index p) and warm population (index h) of the same density with $\beta_h=0.2$. The propagation angle is $\theta=60^\circ$. The oscilliton velocity is $U=0.83V_{Ap}$. The resulting oscilliton frequency is very close to Ω_p . In the last panel of Figure 4c and 4d the hodogram of the electric field (E_z over E_y) and the spatial variation of E_z , respectively, are shown in addition.

1. Harmonic generation

Stimulated by the observation of the harmonics of the EMIC waves, e.g. Usanova et al. (2016), the question has become topical as to whether and in what way the stationary, non-linear structures of oscillitons can be a source of higher harmonics. Surprisingly, the Fourier analysis of the spatial profiles as shown in Figure 4 has produced results that are apparently directly related to the characteristic features of observed harmonics. It turned out that the properties of the harmonics generated by the oscilliton depend crucially on which wave modes are involved in its formation and in which (ω, k) space this occurs. Guided by the observation results of Usanova et al. (2016, 2018), Chen et al. (2018) and Zhu and Chen (2019), we have analyzed three types of harmonic generation associated with oscillitons. In the first case, Figure 5a and 5b, an oscilliton is considered that exists in a proton plasma with 1% admixture of O^+ . At a selected angle $\theta = 10^\circ$, the associated wave number is determined by $kc/p \sim 0.11$, and with an oscilliton velocity of $U = 1.01V_{Ap}$, the fundamental frequency identical with the cross-over frequency is $\omega/\Omega_p = 0.11$. As can be seen from Figure 5b, two further harmonics occur at $kc/p \sim 0.22$ and $kc/p \sim 0.33$, respectively. Accordingly, the frequencies are $\omega/\Omega_p \sim 0.22$ and $\omega/\Omega_p \sim 0.33$.

A different situation arises, shown in Figures 5c and 5d, when as source of EMIC waves an oscilliton is chosen which based on the interaction of two oxygen ion populations at different temperatures. In this case the fundamental frequency of the oscilliton is very close to the oxygen ion cyclotron frequency $\Omega_{O^+} = 0.063\Omega_p$. Starting with the fundamental wave number of $kc/p = 0.07$, in Figure 5d more than 10 harmonics are seen. The spectral maximum at about $kc/p \sim 0.4$ is obviously caused by the existence of another oscilliton (marked by the red dashed circle) which arises due to the momentum coupling between the protons and the oxygen ion populations. Considering the high number of harmonics, one has to take into account that in the fluid approach no cyclotron damping is involved.

Finally, a special case is shown in Figures 5e and 5f, which is related to the fact that the magneto-acoustic mode comes into play assuming finite electron temperatures. Otherwise, the plasma consists of protons with an admixture of 10% He^+ . Here the special situation is shown that, in addition to the previous right- and left-hand polarized modes, the magneto-acoustic mode contributes to the formation of the oscilliton. This is achieved by an appropriate choice of the electron temperature, which is fixed by $T_e = 2.4$, bringing the phase velocity close to $V_{ph}/V_{Ap} = 1$. The special feature of the calculated wave number spectrum in Figure 5f is that only the fundamental wave is electromagnetic in nature and has a corresponding peak in the power spectrum of the magnetic field component (solid line). As can be seen from the dashed curve in Figure 5f, on the other side, several harmonics appear in the power spectrum of the electrostatic field component. Accordingly, these waves are linearly polarized. To what extent magneto-acoustic modes with phase velocities below the Alfvén velocity, due to their coupling with the Alfvén wave, can generate electrostatic harmonics in a similar way has not been further investigated by us. Further discussion follows

later in connection with observations from recent satellite missions.

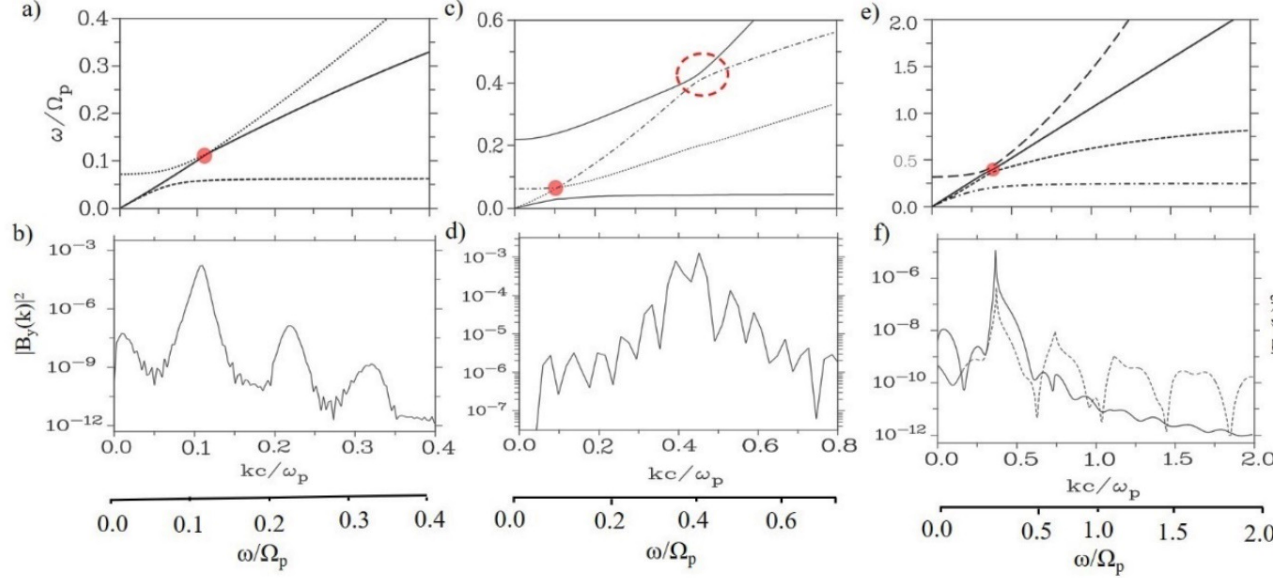


Figure 5. Harmonic generation by three kinds of oscillitons: a, b) oscilliton caused by the momentum exchange between protons and 1% cold oxygen ions; $\beta = 10^0$, $M = U/V_{Ap} = 1.01$; c, d) oscilliton generated in a cold proton plasma with an admixture of 15% cold and 5% hot oxygen ($\beta_h = 0.1$), $U/V_{Ap} = 0.88$; e, f) example of electrostatic cyclotron harmonics illustrating consequences of hot electrons. A plasma with 10% of (cold) He^+ ions is considered; $\beta = 5^0$. With $\beta_e = 2.4$ an electron temperature was chosen that at the cross-over frequency the magneto-acoustic wave (solid line) squeezes itself between both the R- and L-modes. The dispersion (k) of the EMIC waves is shown in the panel a), c) and e). The associated power spectrum the magnetic field component B_y is plotted in the panels below. The dashed curve in panel f) represents the electrostatic field power. The ‘oscilliton frequency’ on the most bottom scale follows from the relation $\omega = k_r \cdot U$. The red points mark the cross-over frequencies.

1. Discussion

It has been shown (Sauer et al. 2001, 2002, 2003a,b; Dubinin et al. 2002, 2003a,b,c) that oscillitons can exist in different plasma systems in which two wave modes are superimposed at one (ω, k) point. These wave modes can be based on the existence of different particle groups, e.g. electrons and ions, beams, electron and ion groups at different temperatures, etc. However, the common property is that the splitting of the associated dispersion curves by mode coupling leaves a gap region in which stationary, growing waves exist. In the end, a non-linear system results in which rotating and/or oscillating groups of particles are resonantly coupled to the electromagnetic field. The properties

of these oscillitons determine the characteristics of the associated coherent waves. In this consideration, the triggering of oscillitons by instabilities initially plays a subordinate role.

So far, it has been difficult to prove this theoretical concept with well-founded measurements. However, this situation has changed with the improved technology and the possibility of multipoint measurements of very recent space missions. In addition, the analysis of low-frequency EMIC waves and the measurement of basic parameters of a multi-ion plasma is easier to realize than details of electron distribution functions when dealing with high-frequency processes, e.g. in the range of whistler and Langmuir waves. In the following we will analyze the various observations about EMIC waves under the aspect, which of their properties can be explained with the concept of oscillitons as presented in Section 2.

The first characteristic quantity of our discussion is the frequency of the EMIC waves. For a magnetospheric multi-ion plasma made of protons (single charged helium and oxygen ions), three emission bands are distinguished: H^+ band between the local H^+ and He^+ cyclotron frequency, He^+ band between the local He^+ and O^+ cyclotron frequency, and O^+ band below the local O^+ cyclotron frequency, see Figure 2. There are numerous measurements that report in particular EMIC waves in the middle of the H^+ band, as by Kim et al. (2015), Vines et al. (2019) and Chen et al. (2020). Statistical analysis of EMIC waves in the H^+ and He^+ band has carried out e.g. by Jun et al. (2019). Triggered EMIC activity in association with Pc1 waves in Cluster measurements has been described by Pickett et al. (2010). Narrow-banded EMIC waves with frequencies at $\sim 0.5\Omega_p$ have also been seen by Temerin and Lysak (1984) in the S3-3 satellite electric field wave data at altitudes between 800 and 8000km. What is striking for EMIC activity in the H^+ band (apart from waves in the immediate vicinity of the proton cyclotron frequency Ω_p) is the absence of frequencies above $\sim 0.5\Omega_p$. This can hardly be explained by a lack of the common proton temperature-anisotropy or beam instability within this frequency range. But it seems to be in accordance with our predictions in Figure 2 according to which the ‘oscilliton frequency’ in the H^+ band (due to a He^+ content) remains below $\sim 0.45\Omega_p$ as long as the corresponding abundance ratio n_{He^+}/n_{H^+} remains below the reasonable value of ~ 0.15 . As an example of statistical measurements by Jun et al. (2019), Figure 2b shows the variation in frequency of EMIC waves in the H^+ and He^+ band over the magnetic latitude (MLAT). From the comparison with Figure 2a one can conclude that the measured maximum frequencies ($\omega/\Omega_p < 0.5$ for the H^+ band, $\omega/\Omega_p < 0.25$ for the He^+ band) are associated with a maximum content of about 20% He^+ and 7% O^+ , respectively. The results of Kim et al. (2015) and Chen et al. (2020) can be commented on in a similar way.

The concept of oscillitons as a source of coherent EMIC waves receives valuable support from the multi-point measurements of the four MMS satellites. With the help of Wave Curl Analysis, Vines et al. (2021) determined the wave num-

ber of a coherent event in the H^+ band with the frequency $\omega/\Omega_p \sim 0.42$. From the measured component parallel to the magnetic field of $k=3.3 \cdot 10^{-3}$ rad/km, a normalized wave number of $kc/v_p \sim 0.5$ is obtained if a proton density (not given in the paper) of $n_p=5\text{cm}^{-3}$ is assumed. With an ‘oscilliton velocity’ of $M=U/V_{Ap} \sim 0.8$ (according to Figure 1a) this results in an ‘oscilliton frequency’ of the EMIC wave of $\sim 0.4 \Omega_p$ which is in good agreement with the spacecraft measurements.

Equally valuable for confirming the oscilliton concept is the evaluation of multi-point measurements by Toledo et al. (2021). According to their ideas, the observed EMIC waves in the H^+ band ($\omega/\Omega_p \sim 0.7$) arise from the momentum exchange of two groups of cold and warm protons via the mediating electromagnetic field. This is shown very convincingly by the measured waveforms for the corresponding proton velocities and the electric and magnetic fields which agree well with the waveforms in Figure 4d. The associated (normalized) wave number is $kc/v_p \sim 1$ and, with a ‘oscilliton velocity’ of $M \sim 1$, supplies an ‘oscilliton frequency’ of $\omega/\Omega_p \sim 1$. EMIC waves in the immediate vicinity of the proton gyro frequency have also been reported by Teng et al. (2019). To what extent, according to our representations, these waves are actually based on the existence of electron groups of different temperatures, however, cannot be inferred from their measurements. The observation of stationary waveforms and the determination of the wave number of EMIC events by is also highlighted in the NASA Report 2017 as a key result of the mission. From the information given there ($\omega=71.5^0$, $k=0.005\text{km}^{-1}$, $\sim 1.9\text{s}^{-1}$, $V_{ph} \sim 373$ km/s) one can conclude that the observed EMIC event is based on the existence of two proton populations whose frequency is close to Ω_p .

The harmonics play a remarkable role in the interpretation of EMIC waves, since their propagation properties allow important conclusions to be drawn about the properties of the plasma and the mechanism by which the fundamental wave is formed. Various observations of electromagnetic ion cyclotron harmonic (EMICH) waves are reported in the literature, These include the work of Liu et al. (1994), Usanova et al. (2016, 2018), Yu et al. (2017), Chen et al. (2018), Zhu and Chen (2019) and Deng et al. (2022). Consistent with our investigations, the events are differentiated by the frequency of the fundamental wave. In some cases this is almost identical to the gyro frequency, in other examples it is above or below it. When considering the relationship between EMICH waves and oscillitons, one must always keep in mind that oscillitons are based on the non-linearity of the fluid-Maxwell equations. It is therefore only natural that the properties of the oscillitons are also reflected in their harmonics.

As first example, the observation of oxygen gyro harmonics by Chen et al. (2018) are discussed. With a frequency of $\sim 1.6 \Omega_{O^+}$ this event corresponds to the theoretical situation in Figure 5a/b where the governing oscilliton arises by the electromagnetic coupling of protons and oxygen at the cross-over point of both mixed modes in the two-ion plasma. The frequencies of the higher harmonics are n times of that of the fundamental wave. The waves propagate nearly parallel to

the magnetic field, $\sim 10^0$, and are linearly polarized which is obviously caused by the superposition of counter-propagating right- and left-handed waves. In the work by Usanova et al. (2016) an EMICH event with frequencies very close to the harmonics of the oxygen ion cyclotron frequency is described. Noteworthy is the observation of a clear change in the direction of wave propagation at the harmonics: the waves with frequencies adjacent to multiples of the O+ gyrofrequency travel on the opposite directions. This event belongs obviously to the case in Figure 5c/4d, where the fundamental wave is an oscilliton which arises due to two coupled oxygen ion populations, consisting of a cold and a warm one. The observed splitting of the harmonics into right-hand and left-hand circular waves propagating in opposite directions suggests a slight drift between the two groups of ions. Another observation by Usanova et al. (2018) of harmonics of the oxygen ion cyclotron frequency Ω_{O^+} , on the other hand, corresponds more to the previously described event of Chen et al. (2018) where the fundamental EMIC wave belongs clearly to the He⁺ band. That means, the frequency of the fundamental wave is above Ω_{O^+} indicating, according our expectations, an oscilliton owing to proton-He⁺ momentum coupling as origin of the observed emission. The quasi-parallel propagation of these waves is considered as a further clue for this interpretation.

In measurements of electromagnetic oxygen ion cyclotron harmonics by Deng et al. (2022) it has been found that the frequencies of these emissions fall around the harmonics of the specific frequency $\omega_0 \sim 2\Omega_{O^+}$. This has stimulated the question whether the second harmonic plays generally a particular role in the nonlinear mechanism of harmonic generation. In this context we want to point out and refer to Figure 4a/b that oscillitons in a proton-He⁺ plasma may generate harmonics whose fundamental frequency ω_0 is approximately $2\Omega_{O^+}$ if the He⁺ content is about 1%. Whether the peculiarity that the oscilliton frequency is actually in the range of the second harmonic of Ω_{O^+} , can only be clarified by appropriate plasma measurements.

With the observation of electrostatic harmonics by Zhu and Chen (2019) a particular type of harmonic generation in association with EMIC waves is reported which is essentially different from the electromagnetic events above. Whereas the fundamental wave is located in the He⁺ band and of electromagnetic nature is, the third harmonic and above (up to fifth) are above the proton cyclotron frequency and have only electric field components (without magnetic fluctuations) propagating bi-directional with respect to the magnetic field. In order to fulfil the resonance conditions (the ω, k relations) a plasma wave mode is required which is essentially electrostatic. In the low-frequency range of EMIC waves that can only be the magneto-acoustic mode with a dispersion of $\omega = C k$, where C is the (constant) phase velocity. Such a case has been considered in our power spectrum analysis of Figure 5e/f. For the selected electron temperature of $T_e = 2.4$ the magneto-acoustic mode with $C = V_{ph} \sim (v_e/2) V_{Ap}$ touches the crossing (oscilliton) point of the proton-He⁺ plasma at $\omega \sim 0.4\Omega_p$ ($kc/v_p \sim 0.4$), see Figure 5e. This condition enables obviously the generation of four and more electrostatic harmonics. Whether electromagnetic coupling between a magneto-acoustic mode

and the Alfvén wave in case $v_e < 2$ ($V_{ph} < 1$) also leads to an oscilliton, that in a similar way may generate electrostatic harmonics, was not further investigated.

A more complex problem concerns the interpretation of the polarization of the observed EMIC waves in relation to our model of oscillitons. It is difficult to derive a consistent picture from the literature. For example, adjacent lines can be polarized differently, as e.g. in the measurements by Chen et al. (2018). However, it remains to be seen that linear polarization is present in the majority of the analyzed events, with left polarization appearing to be somewhat more strongly represented, see Kim et al. (2015), Vines et al. (2019) and Jun et al. (2021). With respect to the polarization of EMIC waves from the spatial oscilliton profiles shown in Figure 4 we have obtained the following results: Oscillitons have both polarizations depending of their velocity U . For positive velocities U they are left-hand polarized with an ellipticity ϵ varying with the plasma parameters between one and zero; commonly is ~ -0.5 . Likewise, oscillitons are right-hand polarized when propagating in the negative direction with respect to the magnetic field. This explains in our view the dominance of linear polarization in the observations which arises from the superposition of triggered oscillitons moving in both directions.

There remains the discussion of the amplitudes of oscillitons. Crucial quantities in the simplest model of the cold multi-ion plasma are the densities of the individual ion components in relation to the proton density. Together with the chosen propagation angle θ they determine the position of the cross-over frequencies and from the dispersion theory of stationary waves $\omega, k=k(U)$, one obtains the spatial growth rates as a function of 'oscilliton velocity' U . From the complete nonlinear theory the spatial profiles of the stationary wave packets, the oscillitons, are determined. In general we have found that oscillitons only exist in a certain range of θ and U . For plausible parameters of the magnetosphere, the optimal range of existence of oscillitons is limited to propagation angles around 15° with the oscilliton velocity U always being limited to the close vicinity of the Alfvén velocity. The amplitudes of oscillitons obtained in this way are generally about one order of magnitude higher than the measured values, see e.g. Teledo et al. (2021) and Vines et al. (2021). In all these considerations, however, one must always keep in mind that the fluid description of its non-linear stationary waves can only represent a very rough model of the real conditions. A first extension could be a kinetic dispersion theory of stationary waves, which could be worked out with reasonable effort. Such an approach would significantly reduce the spatial growth rates from fluid theory values due to kinetic damping effects. Ultimately, you have to use simulations, e.g. in the form of hybrid codes, to check the simple models.

A final but very important point of discussion concerns the role of instabilities in the formation of multi-ion oscillitons as the source of coherent waves in the plasma. In this process they are involved in two ways. In the first case, they are responsible for triggering the oscillitons when the conditions for their existence are present. This means that the instabilities are the reason why the system

of two particle populations and the connecting electromagnetic field starts to oscillate. In the (ω, k) space this happens at the cross-over points, where phase and group velocities are the same. It is worth noting that these points are generally different from those of maximum instability. Another situation occurs when the instability, e.g. due to wave-particle heating, creates a second particle group that differs from the already existing one due to different temperature or speed (e.g. Usanova, 2021). In this case, oscillitons can arise in which groups of particles with the same mass participate, but which differ from each other in other parameters.

1. Conclusions

In conclusion, we would like to express that the described investigations of multi-ion oscillitons in the magnetosphere can be fully transferred to comparable situations in other plasma environments. This applies in particular to the plasmas in the vicinity of comets and non-magnetized planets, where the interaction of the solar wind with the locally generated ions leads to complex wave phenomena in the low-frequency range (Tsurutani, 1991; Nagy et al., 2004 ; Mazelle et al. 2004). But also the solar wind itself is a laboratory for the investigation of multi-ion structures due to its composition of different proton groups (core and halo) and the admixture of alpha particles. In this context, the recent measurements of the Solar Orbiter of coherent proton cyclotron frequency waves of both polarizations (RH and LH) are worth mentioning (Khotyaintsev et al., 2021). Referring to Figures 4c and 4d, the conclusion is obvious that two different proton populations are involved in the formation of the observed stationary nonlinear structures (oscillitons).

Finally, regarding the momentum exchange between electrons, similar conditions can also prevail in the frequency range of the whistler waves and lead to whistler oscillitons (not described so far) if the plasma has several electron groups with different temperatures, maybe produced by the selective effect of temperature-anisotropy instability. This may explain the observed wave packets of whistler waves in the magnetosphere (Dubinin et al., 2007) and in the solar wind (Breneman et al., 2010) and of chorus waves in the magnetosphere (Tsurutani et al., 2009, 2020).

Acknowledgements

The paper is theoretical and does not use external data.

Appendix

1. Hall-MHD equations

The governing system of Hall-MHD equations on which the theory of oscillitons is based is the following, using standard notations:

The continuity equation and equation of motion of ions, p, h and i stands for protons, He⁺ ions and O⁺ ions, respectively.

p_j is the thermal pressure, $p_j = n_j \cdot T_j$.

With the assumption of massless electrons the equation of motion for the electrons is reduced to

The electron density n_e follows via charge neutrality:

$$n_e = n_p + n_h + n_i. \quad (\text{A4})$$

Together with Faraday's law

and Ampere's law

where the current is given by

$$\mathbf{j} = e(n_p \mathbf{v}_p + n_h \mathbf{v}_h + n_i \mathbf{v}_i - n_e \mathbf{v}_e) \quad (\text{A7})$$

one gets a closed system of equations.

1. Oscilliton equations for a cold two-ion plasma

In order to analyse the nonlinear, stationary spatially oscillating structures (oscillitons) which may arise in the frequency gaps near the cross-over points of multi-ion plasmas, a one-dimensional model is considered. The x-axis is in the propagation direction of the wave; the magnetic field is located in the x-z plane with an angle θ with respect to the x-axis, i.e. $\mathbf{B}_0 = (B_0 \cos \theta, 0, B_0 \sin \theta)$. Looking for stationary waves, all variables $f(x,t)$ with respect to the time dependence are considered as function of $x' = x - Ut$: $f = f(x, x - Ut)$ where U is the velocity of the moving structure. Thus, the convective derivative $D/Dt = \partial/\partial t + u_{ix} \partial/\partial x \rightarrow (-U + u_{ix}) \partial/\partial x$.

The resulting system equations which describes the simplest kind of oscillitons in a cold two-ion plasma is given below. The plasma under consideration consists of cold electrons and two cold ion populations, protons (index p) and single-charged helium (index i). All quantities are written in units of the protons, that means $n_i = n_{\text{He}^+} / n_{p0}$ is the normalized He^+ density, where n_{p0} is the undisturbed proton density. The mass is in units of the proton mass m_p , i.e. $m_i = m_{\text{He}^+} / m_p = 4$. The velocities are normalized with the proton Alfvén velocity $V_{Ap} = B_0 / (\mu_0 n_{p0} m_p)^{1/2}$, the magnetic field is in units of B_0 . Thus, the normalized 'oscilliton velocity' is given by $M = U / V_{Ap}$ and the unit of the electric field is $E_0 = V_{Ap} B_0$.

To determine the 17 variables ($n_p, n_i, n_e, \mathbf{v}_p, \mathbf{v}_i, \mathbf{v}_e, B_y, B_z, E_x, E_y, E_z$) our system of equations consists of 6 differential equations and 11 algebraic relations. The latter result either directly from the assumption of massless electrons and charge neutrality or they are the result of the integration of the (stationary) Hall-MHD equations. The system of equations can be written as follows:

$$\frac{dv_{iy}}{dx} = \frac{1}{m_i} \left[\frac{n_{i0} B_z - n_i B_{z0}}{n_{i0}} + \frac{n_i v_{iz} B_x}{n_{i0} M} \right] \quad (\text{B1})$$

$$(\text{B2})$$

$$(\text{B3})$$

(B4)

(B5)

(B7)

(B8)

(B9)

(B10)

(B11)

$$v_{ex} = (n_p v_{px} + n_i v_{ix})/n_e \quad (\text{B12})$$

$$v_{ey} = -\frac{M}{B_x n_e} n_{e0} B_y \quad (\text{B13})$$

$$v_{ez} = -\frac{M}{B_x n_e} (n_{e0} B_z - n_e B_{z0}) \quad (\text{B14})$$

(B15)

(B16)

(B17)

If we fix the He^+ content and the propagation angle θ , the only open parameter is the 'oscilliton velocity' $M=U/V_{Ap}$. From the linearized theory of stationary waves described in Section 2.2, one gets the range of M in which spatially growing waves may occur. For demonstration, a plasma with 10% of He^+ is assumed. Further, a propagation angle of $\theta=12^\circ$ was chosen. In this case, an oscilliton exists for $M=1.06$ and with the related wave number of $kc/p=0.375$ one gets a oscilliton frequency of $\omega/\Omega_p \sim 0.4$. By solving the system of equations B1-B17 the corresponding hodograms and spatial profiles shown in Figure B1 have been obtained.

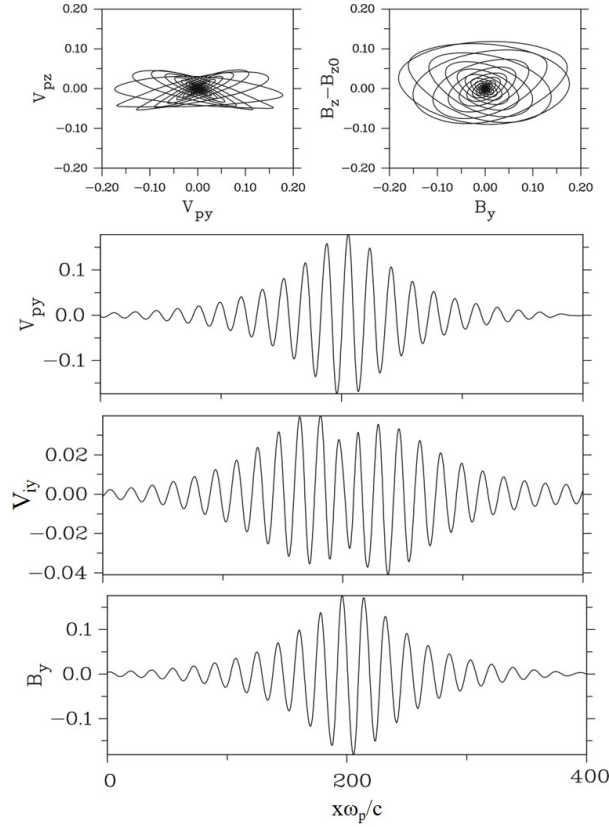


Figure B1. Hodograms and spatial profiles of an oscilliton in a cold proton-He⁺ plasma. The He⁺ abundance ratio is $n_{\text{He}^+} = n_{\text{He}^+} / n_{\text{p}o} = 0.1$. The propagation angle is $\theta = 12^\circ$, the oscilliton velocity is $M = 1.06$. The hodograms of the transverse proton velocity (V_{pz} over V_{py}) and of the transverse magnetic field ($B_z - B_{z0}$ over B_y) are shown in the top two panels. In three panels below the transverse velocities of protons (V_{py}) and He⁺ ions (V_{iy}) and the transverse magnetic field (B_y) versus the spatial coordinate x_p/c are plotted. The characteristic signatures of an oscilliton in form of the spatially oscillating growth and decay are clearly seen.

References

Baumjohann, W., R.A. Treumann, F. Georgeescu, G. Haerendel, K.-H. Fornacon, and U. Auster (1999), Waveform and packet structure of lion roars, *Ann. Geophys.*, 17, 1528.

Breneman, A., C. Cattell, S. Schreiner, K. Kersten, L. B. Wilson III, P. Kellogg, K. Goetz, and L. K. Jian (2010), Observations of large-amplitude, narrow-band whistlers at stream interaction regions, *J. Geophys. Res.*, 115, A08104, doi:10.1029/2009JA014920.

- Dubinin, E., K. Sauer and J.F. McKenzie (2002), Solitons and oscillitons in cold bi-ion plasmas: a parameter study, *J. Plasma Physics*, 68, 27-52.
- Dubinin, E., K. Sauer, and J. F. Mckenzie, and G. Chanteur (2003a), Stationary waves and solitons in a cold p- plasma, *Journal. Geophys. Research*, 108, <https://doi.org/10.1029/2002JA009571>.
- Dubinin, E., K. Sauer, and J. F. Mckenzie, and G. Chanteur (2003b), Solitons, oscillitons, and stationary waves in a warm p- plasma, *Journal of Geophysical Research*, 108, A7, 1293, <https://doi.org/10.1029/2002JA009572>.
- Dubinin, E., K. Sauer, and J. F. Mckenzie (2003c), Nonlinear stationary waves and whistler oscillitons. Exact solutions. *J. Plasma Physics*, 69, 305-330.
- Dubinin, E., K. Sauer, and J. F. Mckenzie (2004), Nonlinear stationary waves and solitons in ion beam-plasma configuration, *Journal of Geophysical Research*, 109, A02208, <https://doi.org/10.1029/2003JA010283>.
- Dubinin, E.M., M. Maksimovic, N. Cornilleau-Wehrin, D. Fontaine, P. Travnicek, A. Mangeney, O. Alexandrova, K. Sauer, M. Fraenz, I. Dandouras, E. Lucek, A. Fazakerley, A. Balogh, and M. Andre (2007), Coherent whistler emissions in the magnetosphere – Cluster Observations, *Ann. Geophys.*, 25, 303–315, www.ann-geophys.net/25/303/2007.
- Chen, Huayue , Xinliang Gao, Quanming Lu, and Shui Wang (2018). In Situ Observations of Harmonic Alfvén Waves and Associated Heavy Ion Heating, *The Astrophysical Journal*, 859:120 (6pp), 2018, June 1; <https://doi.org/10.3847/1538-4357/aabee2>
- Deng, D., Yuan, Z., Huang, S., Xue, Z., Huang, Z., & Yu, X. (2022). Electromagnetic ion cyclotron harmonic waves generated via nonlinear wave-wave couplings. *Geophysical Research Letters*, 49, e2021GL097143. <https://doi.org/10.1029/2021GL097143>.
- Fazakerley, A. N., Coates, A. J., & Dunlop, M. W. (1995). Observations of upstream ions, solar wind ions and electromagnetic waves in the Earth's foreshock. *Advances in Space Research*, 15 (8-9), 103-106.
- Fuselier, S.A., M.F. Thomsen, J.T. Gosling, S.J. Bame, and C.T. Russell (1986), Gyration and intermediate ion distributions upstream from the Earth's bow shock, *Journal of Geophysical Research: Space Physics*, 91 (A1), 91-99.
- Jun, C.-W., Yue, C., Bortnik, J., Lyons, L. R., Nishimura, Y. T., & Kletzing, C. A. (2019). EMIC wave properties associated with and without injections in the inner magnetosphere. *Journal of Geophysical Research: Space Physics*, 124, 2029–2045. <https://doi.org/10.1029/2018JA026279>.
- Jun, C.-W., Miyoshi, Y., Kurita, S., Yue, C., Bortnik, J., Lyons, L., et al. (2021). The characteristics of EMIC waves in the magnetosphere based on the

- Van Allen Probes and Arase observations. *Journal of Geophysical Research: Space Physics*, 126, e2020JA029001. <https://doi.org/10.1029/2020JA029001>.
- McKenzie, J.F., E. Dubinin, K. Sauer and T. Doyle (2004), The application of the constants of motion to nonlinear stationary waves in complex plasmas: a unified fluid dynamic viewpoint, *Journal of Plasma Physics*, 70, 431-462.
- Khotyaintsev, Yu. V., D. B. Graham, A. Vaivads, K. Steinvall, N. J. T. Edberg, A. I. Eriksson, E. P. G. Johansson, L. Sorriso-Valvo, M. Maksimovic, S. D. Bale, T. Chust, V. Krasnoselskikh, M. Kretzschmar, E. Lorfèvre, D. Plettemeier, J. Souček, M. Steller, Š. Štverák, P. Trávníček, A. Vecchio, T. S. Horbury, H. O'Brien, V. Evans and V. Angelini (2021), Density Fluctuations Associated with Turbulence and Waves, First Observations by Solar Orbiter, *Astronomy and Astrophysics*, 656, A19, <https://doi.org/10.1051/0004-6361/202140936>.
- Li, X., and S. R. Habbal (2001), Damping of fast and ion cyclotron oblique waves in the multi-ion fast solar wind, *Journal of Geophysical Research: Space Physics*, 106, 10669-10680, <https://doi.org/10.1029/2000JA000420>.
- Mazelle, C., D. Winterhalter, K. Sauer, J.G. Trotignon et al. (2004), Bow Shock and Upstream Phenomena at Mars, *Space Science Reviews* 111, 115-181.
- Min, K., R. E. Denton, K. Liu, S. P. Gary, and H. E. Spence (2017), Ion Bernstein instability as a possible source of oxygen ion cyclotron harmonic waves, *J. Geophys. Res. Space Physics*, 122, 5449–5465, doi:10.1002/2017JA023979.
- Nagy, A.F. D. Winterhalter, K. Sauer, T.E. Cravens, et al. (2004), The Plasma Environment of Mars, *Space Science Reviews* 111, 33-114.
- Pickett, J.S., B. Grison, Y. Omura, M. J. Engebretson, I. Dandouras, A. Masson, M. L. Adrian, O. Santolík, P. M. E. Décréau, N. Cornilleau-Wehrlin, and D. Constantinescu (2010), Cluster observations of EMIC triggered emissions in association with Pc1 waves near Earth's plasmapause, *Geophys. Res. Letters*, 37, L09104, doi:10.1029/2010GL042648.
- Rauch, J. L., and A. Roux (1982), Ray tracing of ULF waves in a multicomponent magnetospheric plasma: Consequences for the generation mechanism of ion cyclotron waves, *J. Geophys. Res.*, 87, 8191–8198, doi:10.1029/JA087iA10p08191.
- Rubin, M., R. Combi, K. Daldorff, T. Gombosi et al. (2014), Comet 1P/Halley multifluid MHD Model for the Giotto fly-by, *The Astrophysical Journal*, 781:86(13pp), doi:10.1088/0004-637X/781/2/86OC 2014.
- Sauer, K., A. Bogdanov and K. Baumgärtel (1994), Evidence of an ion composition boundary (protonopause) in bi-ion fluid simulations of solar wind mass loading, *Geophys. Res. Letters*, 21, 2255-2258.
- Sauer, K., E. Dubinin, and J.F. McKenzie (2001), New type of soliton in bi-ion plasmas and possible implications, *Geophys. Res. Letters*, 28, 18, 3589-3592, <https://doi.org/10.1029/2001GL013047>.

- Sauer, K., E. Dubinin, and J.F. McKenzie (2002), Wave emission by whistler oscillitons: Application to ‘coherent lion roars’, *Geophys. Res. Letters*, 29, 24, 2226, doi:10.1029/2002GL015771.
- Sauer, K., E. Dubinin, and J. F. McKenzie (2003a), Solitons and oscillitons in multi-ion space plasmas, *Nonlinear Processes in Geophysics*, 10: 121–130. doi: 10.5194/npg-10-121-2003.
- Sauer, K., and E. Dubinin, (2003b), Oscillitons and gyrating ions in a beam-plasma system, *Geophysical Research Letters*, 30, 2192, doi:10.1029/2003GL018266.
- Sauer, K., and Sydora, R. D. (2011). Whistler-Langmuir oscillitons and their relation to auroral hiss. *Ann. Geophys.*, 29(10), 1739–1753. <https://doi.org/10.5194/angeo-29-1739-2011>.
- Sauer, K., and Sydora, R. D. (2012). Mode crossing effects at electron beam plasma interaction and related phenomena. *Plasma Phys. Control. Fusion*, 54(12), 124045. <https://doi.org/10.1088/0741-3335/54/12/124045>.
- Smith, R.L., and N. Brice (1964), Propagation in multicomponent plasma, *Journal Geophysical Research*, 69, 5029-5040.
- Temerin, M., and R.L. Lysak (1984), Electromagnetic Ion Cyclotron Mode (ELF) Waves Generated By Auroral Electron Precipitation, *Journal Geophys. Research*, 89, 2849-2859.
- Teng, S., Li, W., Tao, X., Ma, Q., Wu, Y., Capannolo, L., et al. (2019). Generation and characteristics of unusual high frequency EMIC waves. *Geophysical Research Letters*, 46, 14,230–14,238. <https://doi.org/10.1029/2019GL085220>.
- Thompson, P., M. K. Dougherty and D. J. Southwood (1995), Wave behaviour near critical frequencies in cold bi-ion plasmas, *Planet. Space Sci.*, 43, 5, 625-634.
- Toledo-Redondo, S., Lee, J. H., Vines, S. K., Turner, D. L., Allen, R. C., Andre, M., et al. (2021). Kinetic interaction of cold and hot protons with an oblique EMIC wave near the dayside reconnecting magnetopause. *Geophysical Research Letters*, 48, e2021GL092376. <https://doi.org/10.1029/2021GL092376>.
- Tsurutani, B. T., and Smith, E. J. (1974). Postmidnight chorus: a substorm phenomenon. *J. Geophys. Res.*, 79(1), 118–127. <https://doi.org/10.1029/JA079i001p00118>.
- Tsurutani, B.T.(1991), Comets: a Laboratory for Plasma Waves and Instabilities, in *Cometary Plasma Processes*, Vol. 61, ed. A. Johnstone, <https://doi.org/10.1029/GM061p0189>
- Tsurutani, B. T., Chen, R., Gao, X., Lu, Q., Pickett, J. S., Lakhina, G. S., et al. (2020). Lower-band “monochromatic” chorus riser subelement/wave packet observations. *Journal of Geophysical Research: Space Physics*, 125, e2020JA028090.

<https://doi.org/10.1029/2020JA028090>.

Usanova, M., Malaspina, D., Jaynes, A., Bruder, R., Mann, I., Wygant, J. R., & Ergun, R. (2016). Van Allen probes observations of oxygen cyclotron harmonic waves in the inner magnetosphere. *Geophysical Research Letters*, *43*, 8827–8834. <https://doi.org/10.1002/2016GL070233>.

Usanova, M. E., Ahmadi, N., Malaspina, D. M., Ergun, R. E., Trattner, K. J., Reece, Q., et al. (2018). MMS observations of harmonic electromagnetic ion cyclotron waves. *Geophysical Research Letters*, *45*, 8764–8772. <https://doi.org/10.1029/2018GL079006>.

Usanova, M. E. (2021), Energy Exchange Between Electromagnetic Ion Cyclotron (EMIC) Waves and Thermal Plasma: From Theory to Observations, *Front. Astron. Space Sci.*, *17* <https://doi.org/10.3389/fspas.2021.744344>

Vines, S. K., Allen, R. C., Anderson, B. J., Engebretson, M. J., Fuselier, S. A., Russell, C. T., et al. (2019). EMIC waves in the outer magnetosphere: Observations of an off-equator source region. *Geophysical Research Letters*, *46*, 5707–5716,

<https://doi.org/10.1029/2019GL082152>.

Vines, S. K., Anderson, B. J., Allen, R. C., Denton, R. E., Engebretson, M. J., Johnson, J. R., et al. (2021). Determining EMIC wave vector properties through multi-point measurements: The wave curl analysis. *Journal of Geophysical Research: Space Physics*, *126*, e2020JA028922. <https://doi.org/10.1029/2020JA028922>.

Yao, Jiansheng, Quanming Lu, Xinliang Gao, Jian Zheng, Huayue Chen , Yi Li, and Shui Wang Generation of harmonic Alfvén waves and its implications to heavy ion heating in the solar corona: Hybrid simulations *Phys. Plasmas* **27**, 012901 (2020); <https://doi.org/10.1063/1.5126169>.

Young, D., S. Perraut, A.Roux et al., wave-particle interaction near Ω_{He+} . Propagation of ion-cyclotron waves in He+ -rich plasma, *J. Geophys. Res.*, doi:<https://doi.org/10.1029/JA086iA08p06755>.

Yu XiongDong, Yuan ZhiGang, Wang DeDong, Huang ShiYong, Li HaiMeng, Yu Tao & Qiao Zheng. Oxygen cyclotron harmonic waves observed using Van Allen Probes, *Science China, Earth Sciences*, doi: 10.1007/s11430-016-9024-3.

Zhang, Y., H. Matsumoto, and H. Kojima (1998), Lion roars in the magnetosheath: Geotail observations, *J. Geophys. Res.*, *103*, 4615-4626, <https://doi.org/10.1029/97JA02519>.

Zhang, X.-J., W. Li, R. M. Thorne, V. Angelopoulos, J. Bortnik, C. A. Kletzing, W. S. Kurth, and G. B. Hospodarsky (2016), Statistical distribution of EMIC wave spectra: Observations from Van Allen Probes, *Geophys. Res. Lett.*, *43*, doi:10.1002/2016GL071158.

Zhang, J., V.N. Coffey, M.O. Chandler, S. A. Boardsen, A. A. Saikin, E. M. Mello, C.T. Russel, R. B. Torbert¹, S.A. Fuselier, B.L. Giles, and D.J. Gershman (2017), Properties, propagation, and excitation of EMIC waves observed by MMS: A case study, NASA-Final Report.

Zhu, H., and L. Chen (2019). On the observation of electrostatic harmonics associated with EMIC waves. *Geophysical Research Letters*, *46*. <https://doi.org/10.1029/2019GL085528>.